Validated Predictive Modeling of Antenna Array Directivity,Gain and SNR at 3.6 GHz for 5G Networks

Received: 13 May 2026; Accepted: 17 June 2026 ***Research Article***

Imadeldin Elsayed Elmutasim
Electrical and Electronics Engineering
Universiti Malaysia Pahang Al-Sultan Abdullah UMPSA
Pahang, Malaysia
imad.elmutasim@ieee.org

***Abstract*— Antenna array directivity, vital for RF communication, is explored using 2x2 to 64x64 arrays. Matlab simulations at 3.6 GHz with a 30-degree tilt reveal directivity increases with array size: 6.02 dB (2x2) to 36.12 dB (64x64). SNR also improves, from 125 dB to 155.10 dB. A Random Forest Regressor achieves an R-squared of 0.991, optimizing performance. This study emphasizes the need for directivity optimization in modern wireless antenna designs.**

Keywords*— *antenna directivity; radiation; wireless connection; signal strength

I. INTRODUCTION

In a range of 3 GHz and 30 GHz, frequency encompasses upper extreme of Super High Frequency (SHF) against the lesser extreme of Ultra High Frequency (UHF) on a considerably limited Fresnel zones and expansive directional gain. SHF is known for its high data flow with finer latency to counterbalance the setback in radiation [1][2].

Antenna is a fundamental tool that sends and accepts electromagnetic waves. As a critical component of telecommunication, it plays the transducing role of interchanging electric signals and radio waves on the corresponding functions of receiving and sending information. This sets its employment across various wireless appliances for the usage of mobile networks, satellite communication, broadcasting, and Wi-Fi [3][4].

Dissimilar antennas possess unalike, yet, integral functions across varying telecommunication domains. On one hand, radiating identical signal encompassing all horizontal directions has made omnidirectional antennas a compatible alternative to multi-directional communications, as seen in applications like Dipole antenna of conventional broadcasting and wireless internet router [5][6]. On the other hand. streamlining radio waves toward a designated direction makes Directional Antennas suitable for minimized disruption across uninvolved directions and increased gain, as seen in Yagi, Parabolic and Patch antennas for signal receiving on television, satellite communication, and other systems with beamforming requirement [7][8][9].

Furthermore, antenna elements can be integrated to form antenna array (AR) such as the multiple-input-multiple-output (MIMO) antennas which has been rudimental to contemporary wireless communication via Wi-Fi, as well as the 4G and 5G networks. Serves as a phased array to computerize the handling of beam directivity, data flow, coverage and reliability are enhanced following an increased number of antennas on both ends of outbound and inbound [10][11].

Parameter surrounding technological configuration of antenna subjects the attention for frequency range in which the designed system operates. Different technological contexts then require distinguished frequency range, as seen from the range of 800 MHz and 3.5 GHz for cellular applications, and 2.4 GHz and 5 GHz for Wi-Fi applications [12][13]. Further preference of directed antenna over isotropic antenna lies on the principal consideration for higher gain from the former's capacity in directing undisrupted wave with minimal interference [14]. System effectiveness as measured in decibels (dBi) on both gain and signal radiation, thus, reflects directivity or specified direction of the antenna in radiation focusing against the considerably less directive setup of omnidirectional alternatives [15][16][17].

This is besides the accounting of electric field orientation or polarization in wave radiation towards improving the magnitude of communicating signal between connected outbound and inbound [18][19]. On the peripheral, sustaining angular width of an antenna's main lobe is important within contemporary technological ground for superior directivity that narrows beam width for elevated operational precision and reliability [20][21][22]. This takes into account the aspects of array factor (AF) and element pattern for the established directivity of uniform linear array (ULA) and uniform rectangular array (URA) [23][24]. Reflected in the layout of a parabolic dish, directivity value is enhanced from a directional design that tremendously narrows the main lobe [25].

This paper pursues the investigation of directivity in antenna configuration from a pre-construed frequency of 3.6 GHz. On a tilt antenna element of 30 degree for observed radiation between the x and y surfaces from boresight as adjacent to the x surface, this study aims to compute the effectiveness of antenna arrays in energy focusing toward a designated direction based on dissimilar designs of 2×2, 4×4, 8×8, 16×16, and 64×64 in rows and columns. The remainder of this papers encompasses related algorithmic equations, acquired findings with explanations of each studied antenna array, and conclusive summarization in the second, third and fourth sections, respectively.

II. MATHEMATICAL MODEL

At each designated direction of , directivity D spherically systemizes the radiation intensity to accord its average ratio. The outcome is manifested by [25]:

$$D(\theta, \varphi) = \frac{U(\theta,\varphi)}{Uavg} \tag{1}$$

where $U(\theta, \varphi)$ represents radiation intensity toward the designated direction, and Uavg represents the average radiation intensity that identifies $P_{rad}/4\pi$ with P_{rad} as the total radiated power.

In this case, radiation intensity affiliates each unit area of radiated power toward the designated direction on the expression of:

$$U(\theta,\varphi) = r^2 . P(\theta,\varphi) \quad (2)$$

where $P(\theta,\varphi)$ represents the power density following spatial gap of r distancing the antenna at the direction of (θ,φ). Constituting the fundamental in radiation intensity across the solid angle in entirety, total power as radiated from the antenna P_{rad} is then manifested by:

$$P_{rad} = \int_0^{2\pi} \int_0^{\pi} U(\theta,\varphi) \sin\theta \, d\theta \, d\varphi. \quad (3)$$

The replacing of Uavg in the Equation (1) with Equation (3) consequentially adapts the expression of directivity as:

$$D(\theta,\varphi) = \frac{4\pi \, U(\theta,\varphi)}{Prad}. \quad (4)$$

Following this, the consideration for maximum directivity is equated by:

$$Dmax = max\left(\frac{4\pi \, U(\theta,\varphi)}{Prad}\right), \quad (5)$$

with approximated directivity of the antenna a specific base number of elements being derived by:

$$D \propto N. \quad (6)$$

Such arrangement fixates the parallel between number of elements and magnitude of directivity through an increasingly precise or narrowed main lobe. The approximation is derived by:

$$D \approx 10 \log_{10}(N) \quad (7)$$

with N represents the total elements of each array. The directivity expression can be exemplified on an 8×8 antenna array with 64 total elements through the derived approximation of:

$$D \approx 10 \log_{10}(64) = 10 \times 1.8 = 18 \text{ dB}. \quad (8)$$

Constructive integration of array factors toward designated direction of the main lobe elevates potency across extensive spatiality with growing focus in the energy radiation. The intention of understanding such proficiency propelled simulated outputs across antenna array designs of 2×2 to 64×64 (2×2, 4×4, 8×8, 16×26 and 64×64) in the Matlab software.

On further note, simulating direction for antenna arrays accounts directionality in propagated signal and data rate on the system's extent for effective information transference. This study specifies the widely adopted element spacing of λ/2 as a fractional incorporation to wavelength λ for decreased disruption and increased manageability of the side lobes. The system's data rate is further gauged on existing affiliation between the specified bandwidth and SNR in Shannon capacity based on the expression of:

$$R = B \cdot \log_2(1+\text{SNR}) \quad (9)$$

where B represents the bandwidth at the specification of 100 MHz. Notably, directivity is influential toward SNR Signal to Noise Ratio due to improvements in signal receiving in the designated direction, lost power and encountered noise from the directional gain. Thereupon, incorporation of machine learning mitigates validity issue of current results on 1,000 samples. System's effectiveness from unseen data is concomitantly appraised on steering angles within the range of -90 and 90 degrees, and the pre-construed frequency of 3.6 GHz between separation of 80% and 20% in training and testing data sets to mitigate the possibility of overfitting. In its entirety, implementation of the model followed fit ensemble function in Matlab software for the training of Random Forest Regressor off 50 decision trees, with further estimations that generate the values for Mean Squared Error (MSE), Mean Absolute Error (MAE), and R-squared metrics [26][27].

Algorithm 1

Input:
Array of actual directivity values (in dB)
Array of predicted directivity values (in dB)
Output:
Scatter plot comparing actual and predicted directivity, with a linear fit line
//Step 1: Import or define the data:
{
Array of actual directivity values (dB)
}actual_directivity←Array of actual directivity values (dB)
{
Array of predicted directivity values (dB)
}predicted_directivity←Array of predicted directivity values (dB)
//Step 2: Initialize the plot:
Create a scatter plot of predicted_directivity{predicted_directivity}predicted_directivity vs. actual_directivity{actual_directivity}actual_directivity using blue circles ('o'\text{'o'}'o').
Overlay a scatter plot of actual_directivity{actual_directivity}actual_directivity vs. itself using red crosses ('x'{'x'}'x').
//Step 3: Add labels and title:
Set the x-axis label as "Actual Directivity (dB)".
Set the y-axis label as "Predicted Directivity (dB)".
Set the title as "Comparison of Actual vs. Predicted Directivity".
//Step 4: Add a legend:
Include labels for:
"Predicted Directivity"\text{"Predicted Directivity"}"Predicted Directivity" (blue circles).
"Actual Directivity"\text{"Actual Directivity"}"Actual Directivity" (red crosses).
//Step 5: Enable gridlines:
Activate gridlines to enhance plot readability.
//Step 6: Add a linear fit line:
Compute regression coefficients:
Use least-squares fitting to derive slope and intercept of the line:
fit_line=m·x+b\text{fit_line} = m \cdot x + bfit_line=m·x+b where m is the slope and b is the intercept.
Generate fitted line values for the range of actual_directivity\text{actual_directivity}actual_directivity.
Add the fit line to the plot:
Plot the fit line as a dashed black line ('–k'\text{'--k'}'–k').
//Step 7: Finalize the plot:
Adjust plot aesthetics for clarity, ensuring all elements are visible and distinguishable.

Algorithmic inclusion elevates the scientific rigor of this study, besides improving the consistency and conformity to a research's best practices. Key benefits enclose clarity, adaptability, and comprehensibility of endorsed method toward improved operation reliability and ability to be validated.

III. Result And Discussion

Current findings visually manifest the 2×2, 4×4, 8×8, 16×16 and 64×64 in antenna array designs to enable independent performance appraisal, while divulging modifiable practices to achieve improved directivity, minimized side lobes, or attaining specific radiation layout pattern. On the onset, Figure 1 and Figure 2 separately illustrate the antenna element array and radiation pattern of a 2 rows by 2 columns (2×2) antenna array design.

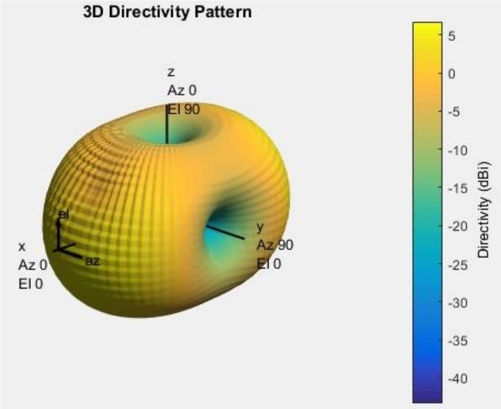

Fig. 1. 2×2 antenna array

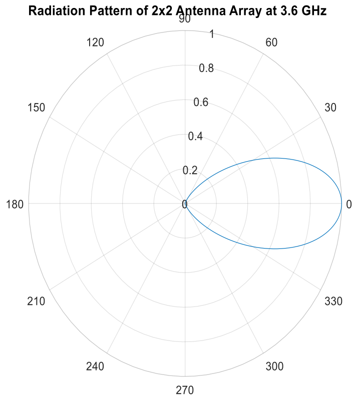

Fig. 2. Radiation Pattern in 2×2 antenna array

The simplistic and cost-effective nature of 2×2 antenna array makes it more preferable for applications in Wi-Fi and other miniature cells. However, it is outperformed by the larger arrays in terms of directivity and capacity, where restricted data stream limits the applications with high data rate requirement. Better performance can be observed from an antenna array design of 4 rows and 4 columns (4×4) as a progressive blueprint through the illustrated elements and radiation pattern in Figure 3 and Figure 4, respectively.

As an improvement in signal quality to the 2×2 antenna array, this design is more reliable. The enhanced data rate, signal quality, and magnitude of wireless network, therefore, idealize the 4×4 antenna array for high usage and operational needs in various urbanized, public and entrepreneurial networks, especially toward the configuration of 4G LTE and 5G NR (New Radio). It is similarly popularized toward numerous complex communication applications such as fixed wireless access and radar systems. Nevertheless, the elements and radiation pattern of a more advanced antenna array design of 8 rows and 8 columns (8×8) can be separately observed in Figure 5 and Figure 6 with an increased antenna directivity.

With a total of 64 elements, the 8×8 antenna array advances other designs with lesser elements on increased gain and directivity, as well as a refinement in spatial multiplexing. Such performance is leveled by its setbacks of increased cost and power usage. However, this is subservient to the 256 elements of the more complex antenna array design of 16 rows and 16 columns (16×16) in Figure 7, following a radiation pattern as observable in Figure 8.

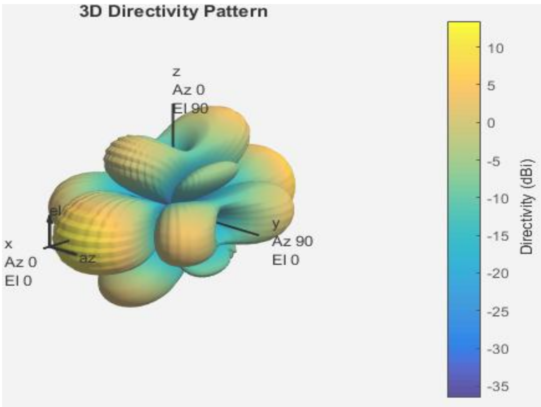

Fig. 3. 4×4 antenna array

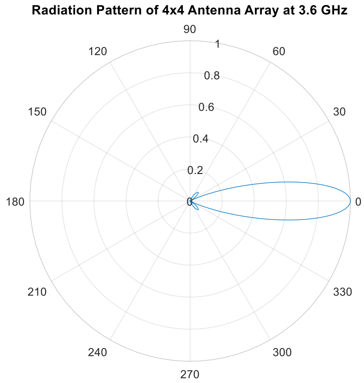

Fig. 4. Radiation Pattern in 4×4 antenna array

This design capitalizes considerable data flow and usage capacity with accurate beamforming to further improve directivity, gain, and spatial resolution in accommodating highly demanding practical applications. Being a critical section of massive MIMO technology in 5G networks, exclusive employment of the 8×8 antenna array on mmWave (millimeter-wave) frequency bands especially exploits the shorter wavelengths to achieve precision in beamforming and increased gain. Practical ability of massive MIMO to concurrently manage heavy traffic and sustain a high data flow, thus, subjects the design's nomination for urbanized and stadium employments on considerable usage capacity. The shortcomings then lie on its increased cost, power consumption, and complexity [10].

Eventually, the most complex design is observed in the 64 rows and 64 columns (64×64) antenna array with a total of 4,096 elements, where the visual configuration and radiation pattern are respectively outlined in Figure 9 and Figure 10.

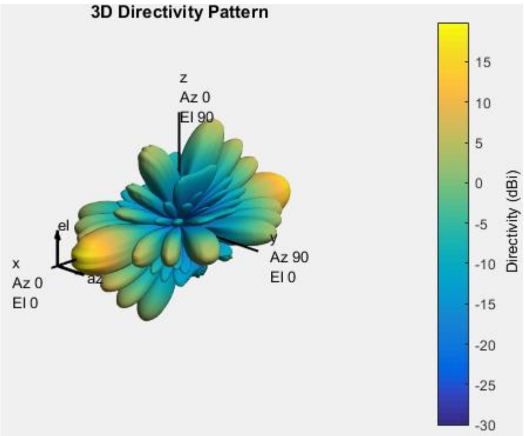

Fig. 5. 8×8 antenna array

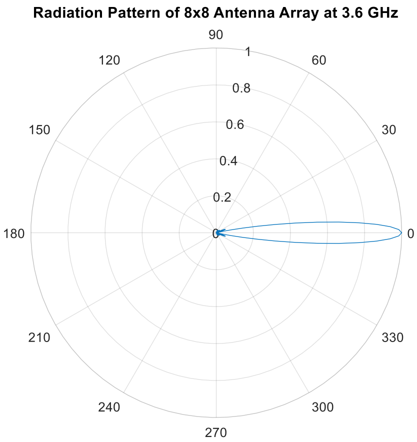

Fig. 6. Radiation Pattern in 8×8 antenna array

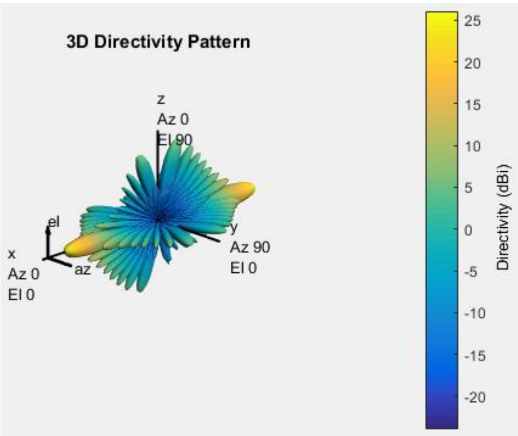

Fig. 7. 16×16 antenna array

As a design that accommodates wireless communications and radar applications with paramount requirement, the design's errorless handling of radiation pattern is idealized for fundamental components of the 5G and the upcoming 6G networks like the ultra-reliable, low-latency communication (URLLC). Additional applications enclose cardinal domains that require timely and reliable information transference such as remote surgery, self-driving automobiles, smart manufacturing, and automated industrialization. However, setbacks remain on the lack of cost effectiveness and operational simplicity [28].

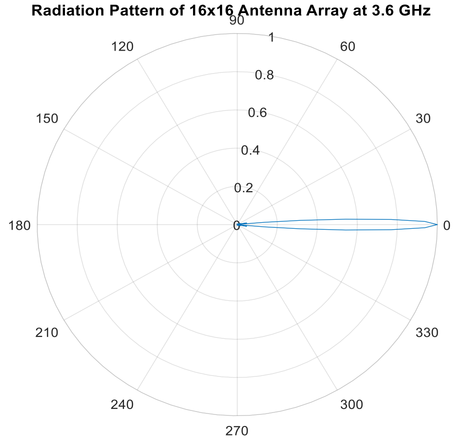

Fig. 8. Radiation Pattern in 16×16 antenna array

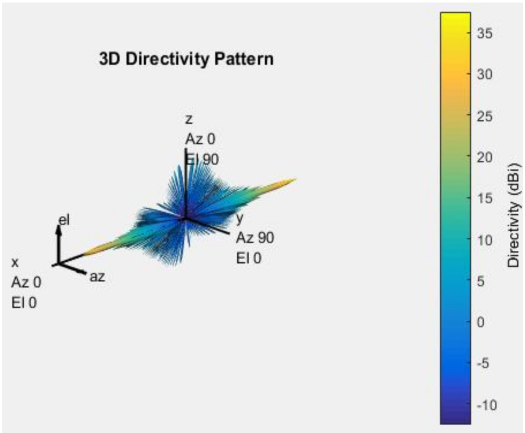

Fig. 9. 64×64 antenna array

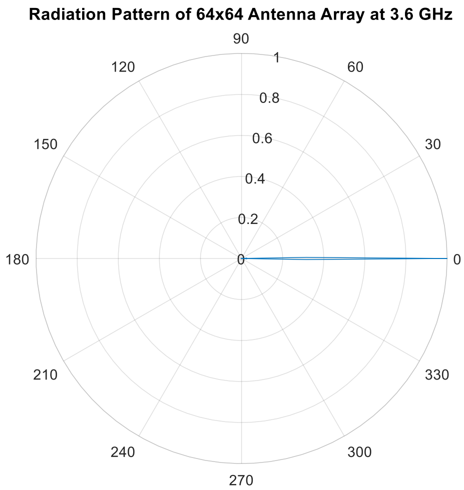

Fig. 10. Radiation Pattern in 64×64 antenna array

TABLE I. ANTENNA ARRAY CALCULATIONS

Antenna array elements	Antenna Directivity in dB	No. of Side Lobes	Achievable SNR in dB
2×2	6.02	0	125.00
4×4	12.04	2	131.02
8×8	18.06	6	137.04
16×16	24.08	14	143.06
64×64	36.12	62	155.10

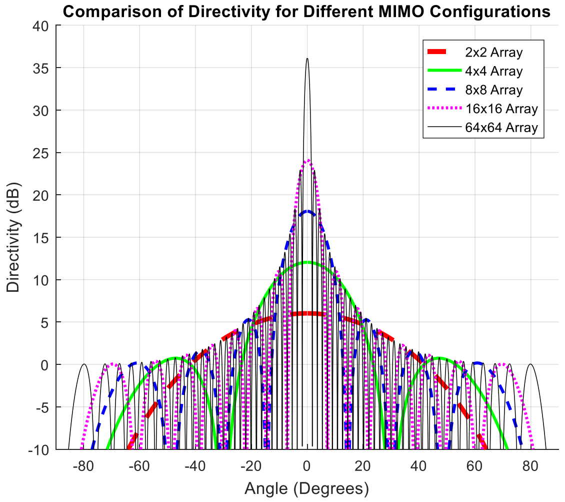

Fig. 11. A comparison directivity for 2×2, 4×4, 8×8, 16×16, and 64×64 antenna arrays

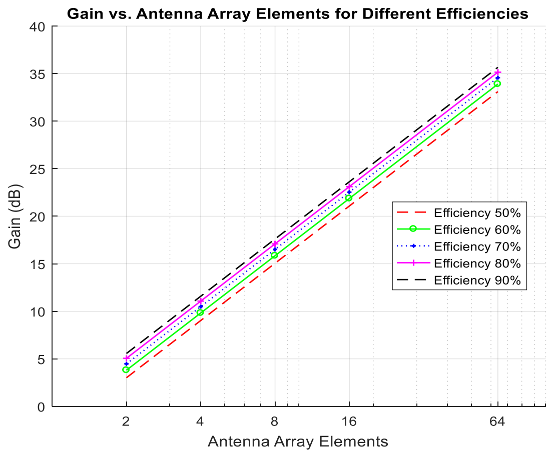

Fig. 12. A comparison gains in dBi for 2×2, 4×4, 8×8, 16×16, and 64×64 antenna arrays

Calculations for the model power rational directivity from the explained antenna array designs are tabulated in Table 1 based on the dBi measurement. Produced results show increased directivity with increasing number of elements. From the absence of side lobe for 2×2 antenna array, it is formed and multiplied on a trend of 2, 6, 14 and 62 for the respective configurations of a 4×4, 8×8, 16×16 and 64×64 rectangular arrays. With pattern of plotted array factors as a reference, the smallest antenna array of 2×2 can be readily used to estimate the total side lobes of larger rectangular N×N (2, 4, 8, 16…) arrays. Progressively, Figure 11 compares the directivities alongside the increasing number of side lobes across the explained antenna array types.

Illustrated comparison based on the explained antenna array designs demonstrates an approximate upward shift of 6 dB in directivity on a factorial increase of 4 in array size. A consistent 6.02 dB in directivity increase is ultimately shown across the intermittent transitions of 2×2, 4×4, 8×8, 16×16, and 64×64 antenna array configurations. Moreover, attainable gain G of each array antenna design with accordance to the respective directivities is outlined in Figure 12.

Gain G is derived from a simplistic formula of $D = G - L$, where D represents the directivity, L represents the lost dBi from the antenna's inefficiency, with consideration for the relationship between efficiency τ and L $(L=10 \log10 (\tau))$. This produces the gain values in dBi from dissimilar efficiency levels, as tabulated in Table 2.

As an extension, the previously mentioned factorial configurations (factorial increase of 4) surmise an intermittent increase of 6 dB in directivity and gain across the antenna array designs. With the ability of antenna directivity system in accommodating an immense usage capacity, the idealization of antenna arrays with higher number of elements to demanding environmental and practical domains is established out of the need for intense data flow. The designs should also mitigate the defiance from emerging usage of mmWave and THz bands on a high directivity, narrowed beam and information transference over distanced locations.

Additionally, performances of each antenna design are contrasted and optimized based on the inclusion of machine learning (ML). Random Forest Regressor was used to appropriate the approach's ensemble learning method with Bagging (Bootstrap Aggregating) as a variation of supervised learning [29][30][31]. The outputs are shown in Figure 13.

An aggregate outlook toward ML estimations and conventional simulations accelerates appraisal to further provide supporting knowledge on the operational compatibility between antenna array designs and the criterion of 3.6 GHz. A significant correlation on estimated to actual directivities can then be concluded on a highly accurate estimation with Mean Squared Error (MSE) of 0.906, Mean Absolute Error (MAE) of 0.756, and R-squared (R2) of 0.991.

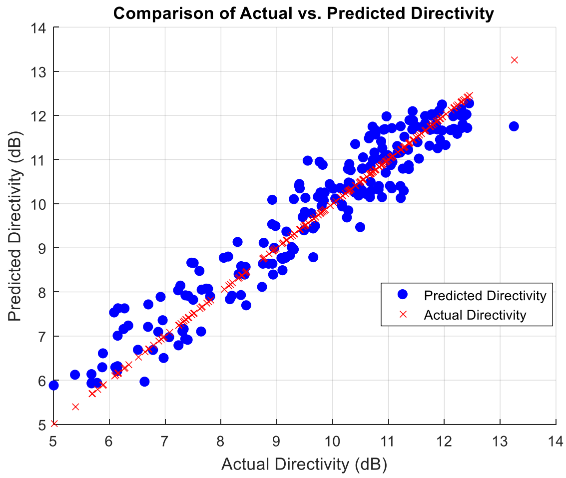

Fig. 13. A comparison between actual and predicted directivity

TABLE II. ANTENNA GAIN CALCULATIONS IN DIFFERENT EFFICIENCIES

Antenna array elements	Efficiency in dB				
	50%	*60%*	*70%*	*80%*	*90%*
2×2	3.01	4.22	5.15	5.95	6.47
4×4	9.03	10.24	11.17	11.97	12.49
8×8	15.05	16.26	17.19	17.99	18.51
16×16	21.07	22.28	23.21	24.01	24.53
64×64	33.11	34.32	35.25	36.05	36.57

IV. Study Validation

Validation is important to a study in confirming the reliability, authenticity and credibility of yielded results. In particular, undertaken statistical and rigorous comparison of current results against previous scholars corroborates increases the integrity merits of the former, while buttressing its scientific contribution. This is contemporaneously done against the results by [32] on the comparable groundworks in elements and frequencies of antenna arrays through the evaluation of antenna directivity and gain. The results for both antenna directivity and gain are separately contrasted in Figure 14 and Figure 15.

On similar parameters, [32] produces the directivities of 7.06 dB, 13.48 dB, 19.71 dB, 25.8 dB, and 38.8 dB for the respective designs of 2×2, 4×4, 8×8, 16×16, and 64×64 in antenna arrays. Whereas, it generates the independent gains of 6.64 dB, 12.67 dB, 18.53 dB, 24.33 dB, and 36.51 dB from these increasing antenna arrays. A between-results validity of 50% to 90%, therefore, confirms exceptional reliability to the findings of this study.

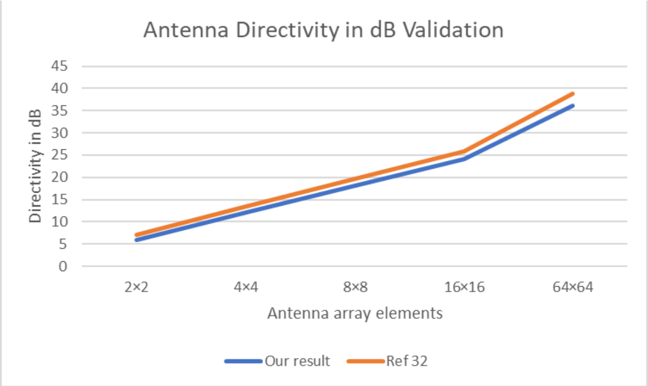

Fig. 14. A comparison between our result and Reference [32] in antenna directivity

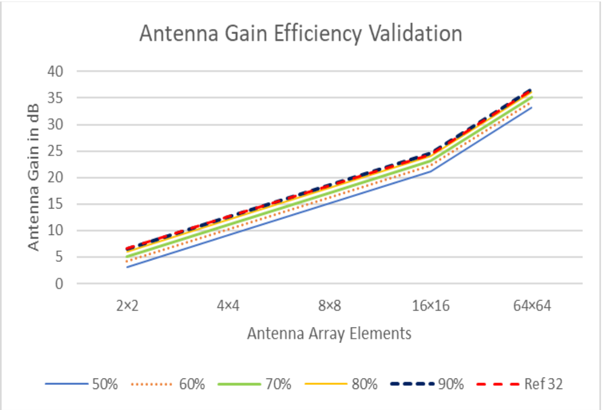

Fig. 15. A comparison between our result and Reference [32] in antenna gain

V. Conclusion

As a centralized tool in telecommunication for the wireless transference and receiving of information throughout different channels, the proliferation of antennas demands contemporary attuning of directivity to a number of communicational requirements such as broadcasted channels and satellite connections that capitalize capacity of the post-5G era. More advanced logarithm from an increased number of antenna array elements could handle the forthcoming challenge of THz bands from a narrowed beam. Findings on a higher number of side lobes and increased directivity from 16×16 and 64×64 antenna array designs over their lesser configurations (2×2 and 4×4) engender precision in beamforming from an increasingly focused radiation pattern for applications like 5G, radar, and satellite systems. Such outcome has been compared against previous scholar on similar grounds, where reliability and validity hold. Upcoming studies can potentially explore the pragmatic optimization of artificial intelligence (AI) algorithms in response to the progressive tapestry.

References

[1] Yamaguchi, S., Nakamizo, H., Shinjo, S., Tsutsumi, K., Fukasawa, T., & Miyashita, H. (2017, July). Development of active phased array antenna for high SHF wideband massive MIMO in 5G. In 2017 IEEE International Symposium on Antennas and Propagation & USNC/URSI National Radio Science Meeting (pp. 1463-1464). IEEE.

[2] Teixeira, E., Sousa, S., Velez, F. J., & Peha, J. M. (2021). Impact of the propagation model on the capacity in small-cell networks: Comparison between the UHF/SHF and the millimeter wavebands. Radio Science, 56(5), 1-13.

[3] Ojaroudi Parchin, N., Jahanbakhsh Basherlou, H., Al-Yasir, Y. I., Abd-Alhameed, R. A., Abdulkhaleq, A. M., & Noras, J. M. (2019). Recent developments of reconfigurable antennas for current and future wireless communication systems. Electronics, 8(2), 128.

[4] Gharode, D., Nella, A., & Rajagopal, M. (2021). State‐of‐art design aspects of wearable, mobile, and flexible antennas for modern communication wireless systems. International Journal of Communication Systems, 34(15), e4934.

[5] Savitri, D. I., Azzahra, A. A., Wulandari, P., & Rahmatia, S. (2018, November). Comparison between hollow aluminum yagi-uda and dipole antenna for indoor antenna TV. In IOP Conference series: Materials science and Engineering (Vol. 453, No. 1, p. 012034). IOP Publishing.

[6] Vithanawasam, C. K. (2021). Design and analysis of TVWS antenna for rural wireless connectivity (Doctoral dissertation, Swinburne).

[7] Kumar, A., & Singh, D. K. (2020, July). Improvement in Gain of Dipole and Yagi-uda Based microstrip fed patch Antenna. In 2020 IEEE International Conference on Electronics, Computing and Communication Technologies (CONECCT) (pp. 1-5). IEEE.

[8] Hua, Z., Haichuan, G., Hongmei, L., Beijia, L., Guanjun, L., & Qun, W. (2015, November). A novel high-gain quasi-Yagi antenna with a parabolic reflector. In 2015 International Symposium on Antennas and Propagation (ISAP) (pp. 1-3). IEEE.

[9] Oliveira, T. E., Reis, J. R., & Caldeirinha, R. F. (2021). Quasi-Yagi microstrip dipole antenna with circular arc parasitic elements for wireless sensing networks. URSI Radio Science Bulletin, 2021(378), 44-50.

[10] Elmutasim, I. (2023). A brief review of massive MIMO technology for the next generation. Int. Arab J. Inf. Technol., 20(2), 262-269.

[11] Wang, Z., Zhang, J., Du, H., Niyato, D., Cui, S., Ai, B., ... & Poor, H. V. (2024). A tutorial on extremely large-scale MIMO for 6G: Fundamentals, signal processing, and applications. IEEE Communications Surveys & Tutorials.

[12] Okaya, T., & Kobayashi, K. (2024, August). Accuracy Comparison of Indoor Positioning of a Drone Base Station Using Wi-Fi RTT in 2.4 GHz and 5 GHz Bands. In 2024 IEEE VTS Asia Pacific Wireless Communications Symposium (APWCS) (pp. 1-5). IEEE.

[13] Yunanta, R. E. C., & Susyanto, T. (2024). Analysis of WiFi Reliability at 2.4 GHz and 5 GHz Frequencies in the Environment of STMIK Sinar Nusantara Surakarta. MALCOM: Indonesian Journal of Machine Learning and Computer Science, 4(3), 1130-1138.

[14] Wang, Y., Tang, M. C., Li, M., Li, D., & Zeng, X. (2024). Planar Single-Layer Wideband Electrically Small Quasi-Isotropic Antenna Characterized by Filtering Response. IEEE Transactions on Antennas and Propagation.

[15] Wu, S. T., Zhang, S. Q., & Wong, S. W. (2024). Compact Broadband High Directivity Omnidirectional Stripline Antenna Array. IEEE Antennas and Wireless Propagation Letters.

[16] Tang, Y., Zhou, Q., Pan, Y., Lü, X., & Wang, X. (2024). Experimental Study of Omnidirectional Scattering Characteristics of Complex Scale Targets Based on Coded Signals. Journal of Marine Science and Engineering, 12(9), 1590.

[17] Chojnacki, B. (2024). Dispersion Influence of Electroacoustic Transducer Parameters in the Design Process of Miniature Loudspeaker Arrays and Omnidirectional Sound Sources. Sensors, 24(15), 4958.

[18] Hamlbar Gerami, H., Kazemi, R., & Fathy, A. E. (2024). Development of a metasurface-based slot antenna for 5G MIMO applications with minimized cross-polarization and stable radiation patterns through mode manipulation. Scientific Reports, 14(1), 8016.

[19] Kiani, N., Tavakkol Hamedani, F., & Rezaei, P. (2024). Switchable circular polarization in flower-shaped reconfigurable graphene-based THz microstrip patch antenna. Analog Integrated Circuits and Signal Processing, 118(2), 259-270.

[20] You, C., Cai, Y., Liu, Y., Di Renzo, M., Duman, T. M., Yener, A., & Swindlehurst, A. L. (2024). Next Generation Advanced Transceiver Technologies for 6G. arXiv preprint arXiv:2403.16458.

[21] Dwivedi, S. (2024). Antenna Design for Beyond 5G: 5G and 6G Applications With Different Materials and Techniques Including Metamaterials and Metasurfaces. In Electromagnetic Wave Control Techniques of Metasurfaces and Metamaterials (pp. 106-140). IGI Global.

[22] Zhang, J., Miao, H., Tang, P., Tian, L., & Liu, G. (2024). New mid-band for 6G: Several considerations from the channel propagation characteristics perspective. IEEE Communications Magazine.

[23] Khalafalla, M., Jiang, K., Tian, K., Feng, H., Xiong, Y., & Tang, B. (2024, May). Radiation Pattern Analysis of the Pentagram Array. In 2024 7th International Conference on Electronics Technology (ICET) (pp. 755-759). IEEE.

[24] Elmutasim, I. E., Mohd, I. I., & Karim, M. S. A. (2023). A New Predictive Hypothesis for Phase Difference Reflection in GHz. Environmental Sciences Proceedings, 27(1), 12.

[25] Khalaj-Amirhosseini, M. (2024). Synthesis of antenna arrays with main lobe and sidelobes of arbitrary levels and widths. International Journal of Electronics Letters, 12(4), 422–434. https://doi.org/10.1080/21681724.2024.2340599

[26] Del Galdo, G., Lotze, J., Landmann, M., & Haardt, M. (2006, September). Modelling and manipulation of polarimetric antenna beam patterns via spherical harmonics. In 2006 14th European Signal Processing Conference (pp. 1-5). IEEE.

[27] Tatachar, Abhishek V. "Comparative assessment of regression models based on model evaluation metrics." International Journal of Innovative Technology and Exploring Engineering 8.9 (2021): 853-860.

[28] D. Kim, J. Hirokawa, M. Ando, J. Takeuchi and A. Hirata, "64× 64-Element and 32× 32-Element Slot Array Antennas Using Double-Layer Hollow-Waveguide Corporate-Feed in the 120 GHz Band," in IEEE Transactions on Antennas and Propagation, vol. 62, no. 3, pp. 1507-1512, March 2014, doi: 10.1109/TAP.2013.2296318.

[29] El Mrabet, Zakaria, et al. "Random forest regressor-based approach for detecting fault location and duration in power systems." Sensors 22.2 (2022): 458.

[30] Lee, Tae-Hwy, Aman Ullah, and Ran Wang. "Bootstrap aggregating and random forest." Macroeconomic forecasting in the era of big data: Theory and practice (2020): 389-429.

[31] J. Jeyasoundari, S. Sridevi and S. C. Raja, "Comparison of Supervised Machine Learning Algorithms with Bagged-Ensemble Method for Intrusion Detection," 2024 IEEE Students Conference on Engineering and Systems (SCES), Prayagraj, India, 2024, pp. 1-6, doi: 10.1109/SCES61914.2024.10652494.

[32] A. H. M. Z. Alam et al., "Scalability Analysis for Designing Large-Scale Antenna Array Using Sub-Array," 2018 7th International Conference on Computer and Communication Engineering (ICCCE), Kuala Lumpur, Malaysia, 2018, pp. 29-33, doi: 10.1109/ICCCE.2018.8539309.